

THE HOT ISM OF THE ANTENNAE OBSERVED WITH CHANDRA: DISCOVERY OF CHEMICAL ENRICHMENT

A. Baldi¹, J. Raymond¹, G. Fabbiano¹, A. Zezas¹, A. Rots¹, F. Schweizer², A. King³, and T. Ponman⁴

¹Harvard-Smithsonian Center for Astrophysics, 60 Garden Street, Cambridge, MA 02138, USA

²Carnegie Observatories, 813 Santa Barbara Street, Pasadena, CA 91101, USA

³Theoretical Astrophysics Group, University of Leicester, Leicester LE1 7RH, UK

⁴School of Physics & Astronomy, University of Birmingham, Birmingham B15 2TT, UK

ABSTRACT

An analysis of the properties of the hot ISM in the merging pair of galaxies known as The Antennae (NGC 4038/39), performed using the deep 411 ks Chandra ACIS-S data set is presented. These deep observations and Chandra’s high angular resolution allow us to investigate the properties of the hot ISM with unprecedented spatial and spectral resolution. Through a spatially resolved spectral analysis, we find a variety of temperatures (0.3–0.7 keV), densities (3×10^{-2} – $1.5 \times 10^{-1} \text{ cm}^{-3}$), and N_H (up to $2 \times 10^{21} \text{ cm}^{-2}$). Metal abundances for Ne, Mg, Si, and Fe vary dramatically throughout the ISM from sub-solar values (~ 0.2) up to ~ 20 times the solar abundance. Comparison of the abundances with the average stellar yields predicted by theoretical models of SN explosions points to Type II SNe as the main contributors of metals to the hot ISM. No evidence of correlation between radiooptical star formation indicators and the metal abundances is found. Although uncertainties in the average density cannot exclude that mixing may have played some important role, the time required to produce the observed metal masses (~ 3 Myr) suggests that the correlations are unlikely to be destroyed by the presence of efficient mixing. More likely a significant fraction of Type II SNe ejecta may be in a cool phase, in grains, or escaping in the wind.

Key words: galaxies: peculiar; galaxies: individual(NGC4038/39); galaxies: interactions; X-rays: galaxies; X-rays: ISM.

1. INTRODUCTION

Massive stars deeply influence the baryonic component of the Universe. Their ionizing radiation and the supernovae (SNe) return kinetic energy and metal-enriched gas to the interstellar medium (ISM) from which the stars

formed (a process called “feedback”). Feedback exercises an influence not only on the gas-phase conditions in the immediate environment of the clusters hosting massive stars (e.g. Pudritz & Fiege 2000), but also on the phase structure and energetics of the ISM on galactic scales (e.g. McKee & Ostriker 1977) and on the thermodynamics and enrichment of the intergalactic medium (IGM) on scales of several Mpc (e.g. Heckman 1999). The vast range of spatial scales involved is only one of the difficulties encountered in attempting to study feedback. Even restricting the discussion to purely mechanical feedback from SNe and stellar winds (SN feedback), another difficulty is the broad range of complicated gas-phase physics, which includes (magneto)hydrodynamic effects such as shocks and turbulence, thermal conduction, and non-ionization equilibrium (NEI) emission processes.

Several attempts at putting quantitative constraints on the metal enrichment caused by SN feedback in starburst galaxies have been made in the recent past. From a small sample of edge-on starburst galaxies observed by ROSAT and ASCA, Weaver, Heckman, & Dahlem (2000) obtained abundances completely consistent with solar values and no evidence of super-solar ratios of the α elements with respect to Fe, as required by type-II SN feedback (e.g., Gibson, Lowenstein, & Mushotzky 1997). Moreover, they concluded that the technique of measuring abundances through X-ray spectral fitting is highly uncertain because of ambiguities in the fits (e.g., a degeneracy between the temperature and metallicity), and strongly dependent on the model choice (see also Dahlem et al. 2000; Strickland et al. 2002, 2004). The advent of Chandra, with its sub-arcsecond angular resolution, allowed a better subtraction of the point sources from the galactic diffuse emission, simplifying the spectral fitting. However, the low resolution spectra of the Chandra ACIS CCDs (Weisskopf et al. 1996) did not allow a dramatic improvement in the accuracy of abundance measures. Notwithstanding the limits of ACIS spectral resolution, Martin, Kobulnicky, & Heckman (2002), observing the dwarf starburst galaxy NGC 1569, claimed to obtain ratios of α elements to Fe 2–4 times higher than

the solar value.

While X-ray observations of the halos of nearby edge-on disk galaxies may provide the best single probe of the action of mechanical feedback on galactic scales, observations of the disks of *face-on* nearby spiral galaxies may provide useful insights into the physics and enrichment of the hot gas. Such observations allow a spatially resolved analysis of the hot ISM in the disk that is much less affected by internal absorption than in the case of edge-on galaxies.

The Antennae are the nearest pair of colliding, relatively face-on spiral galaxies involved in a major merger ($D = 19$ Mpc for $H_0 = 75 \text{ km s}^{-1} \text{ Mpc}^{-1}$). Hence, this system not only allows a study of the properties of the ISM relatively unaffected by internal absorption, but it also provides a unique opportunity to get the most detailed insight possible into the consequences of a galaxy merger, such as induced star formation and its effect on the ISM. The presence of an abundant hot ISM in The Antennae was originally suggested by the first *Einstein* observations of this system (Fabbiano & Trinchieri 1983), and has since been confirmed by observations with several major X-ray telescopes (*ROSAT*: Read, Ponman, & Wolstencroft 1995, Fabbiano, Schweizer, & Mackie 1997; and *ASCA*: Sansom et al. 1996). The first *Chandra* ACIS observation of The Antennae in 1999 gave us for the first time a detailed look at this hot ISM, revealing a complex, diffuse, and soft emission component responsible for about half of the detected X-ray photons from the two merging galaxies (Fabbiano, Zezas & Murray 2001; Fabbiano et al. 2003, hereafter F03). The spatial resolution of *Chandra* is at least 10 times superior to that of any previous X-ray observatory, which allows us to resolve the emission on physical scales of ~ 75 pc (for $D=19$ Mpc) and to detect and subtract individual point-like sources (most likely X-ray binaries; see Zezas et al. 2002).

While the first *Chandra* data set demonstrated the richness of the ISM in The Antennae, the number of detected photons was insufficient to study its detailed small-scale morphology and spectral properties. A deep monitoring observing campaign of The Antennae with *Chandra* ACIS has produced a detailed and rich data set. This data-set revealed a complex diffuse emission, with signatures of strong line emission coming from some of the hot ISM regions, pointing to high α element abundances (Fabbiano et al. 2004, Baldi et al. 2005a,b). Here we resume the physical properties of the hot gas and we investigate its enrichment by SN explosions.

2. IMAGING AND SPECTRAL ANALYSIS

NGC 4038/39 was observed with *Chandra* ACIS-S seven times during the period between December 1999 and November 2002, for a total of ~ 411 ks. The data products were analyzed with the CXC CIAO v3.0.1 software and XSPEC package. Full details about the data processing and reduction are given in Baldi et al. (2005a, hereafter Paper I).

Paper I presents a mapped-color image of the diffuse emission in The Antennae, representing contributions

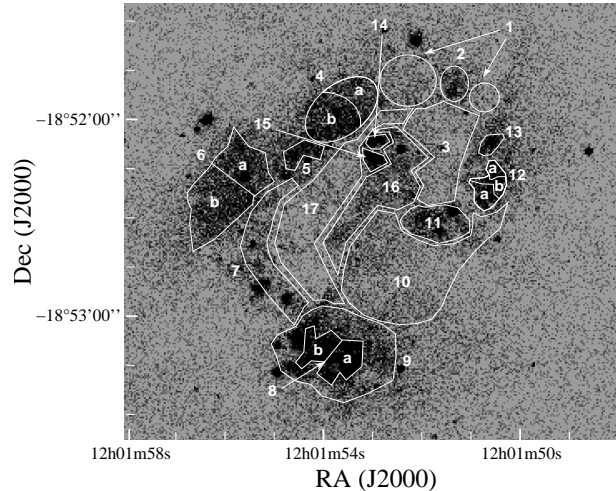


Figure 1. 0.3–6 keV *Chandra* ACIS-S image of The Antennae. The 21 regions used for the spectral analysis of the hot ISM are marked in white. A high-resolution color version of this figure can be found in Paper I.

from three different energy bands: 0.3–0.65 keV, 0.65–1.5 keV and 1.5–6 keV. Before combining the images from the three bands, all point sources were subtracted and an adaptive gaussian kernel was applied to each of the three images. A similar procedure was applied to generate a line-strength map for the emission lines from O+Fe+Ne (0.6–1.16 keV), Mg (1.27–1.38 keV), and Si (1.75–1.95 keV) in different regions of the hot ISM.

Both the mapped-color image of the diffuse emission and the line-strength map (presented in Figure 4 and 6 of Paper I) guided us in selecting 21 spectrally similar regions for a proper spectral analysis. These regions are shown in Figure 1. The method used for the spectral extraction and analysis is fully described in Paper I.

Almost all regions could be fitted with a single thermal component. Only Region 4b required two thermal components with different kT ; in this region, we could not constrain the low kT value (although we found a minimum in the χ^2 statistics at $kT = 0.20$ keV), and we could put only a lower limit ($kT > 0.54$ keV) to the higher temperature component. Almost all the single-temperature regions required a temperature of $kT \sim 0.6$ keV to fit the data, except for regions 5, 8b, and 14 ($kT \sim 0.3$ keV). Considering all the regions analyzed, the temperatures (both in the single- and two-temperature cases) range from ~ 0.2 to ~ 0.8 keV (including the errors). Our analysis yielded metal abundances that have acceptable constraints in the majority of regions, and led to the most important, and somewhat unexpected, result of our spectral analysis: the abundances of Silicon and Magnesium cover a wide range of values ranging from the very low values found in regions 2, 6a, 12a, and 12b ($Z \sim 0.2 Z_\odot$) to the very high values observed in Region 5 ($Z \sim 10$ – $20 Z_\odot$). The intrinsic absorption throughout the hot ISM is generally low, with $N_H \sim 10^{20} \text{ cm}^{-2}$ typical and often consistent with zero. The exceptions are the southern nucleus (regions 8a and 8b) and Region 7, which is significantly obscured also in the optical. In the optical and

near infrared, Region 7 corresponds to the ‘‘Overlap Region,’’ where the most active star formation is now occurring (Mirabel et al. 1998; Wilson et al. 2000; Zhang, Fall, & Whitmore 2001). These three regions show intrinsic absorption of $\sim 1 - 2 \times 10^{21} \text{ cm}^{-2}$.

3. HOT-GAS PARAMETERS

From the parameters determined from the spectral fits we estimated various properties of the emitting plasma, such as electron density n_e ($\approx n_H$), thermal energy content E_{th} , cooling time τ_c , and pressure p . Since we observe regions projected on the plane of the sky, we can only measure the ‘‘footprint’’ of each emitting region. To estimate the emitting volumes we adopted the following procedure. For all ‘‘single’’-temperature regions, we assumed a depth of 200 pc for the emitting volume, corresponding to the typical depth of a spiral disk. In the case of Region 4b, where we have two temperatures, we assumed that the high- and low-temperature components are in pressure equilibrium, and derived the thicknesses for the volumes occupied by these two phases from the best-fit kT s, imposing the condition that they add up to a total value of 200 K pc. The filling factor η is assumed to be unity in our calculations. A filling factor η close to unity for the hot phase of the ISM is plausible from recent results coming from 3D hydrodynamical simulations (η ranging between 0.17 and 0.44 for SN rate between Galactic and 16 times the Galactic value; see, e.g., de Avillez & Breitschwerdt 2004 and references therein). However, our parameters have only a slight dependence on it ($\propto \eta^{-1/2}$ or $\propto \eta^{1/2}$), hence our estimates are precise within a factor of two or less.

The calculated cooling times are in the 10^7 – 10^8 yr range and in agreement with the results of F03. The pressure is generally of the order of a few 10^{-11} dyne cm^{-2} , but reaches higher values (a few 10^{-10} dyne cm^{-2}) in the two nuclei and also in the regions corresponding to the hot-spot regions R1 and R2 of F03. These new values are in excess of those found in F03, possibly reflecting the fact that larger areas were averaged over in that work. F03 argued for a possible pressure equilibrium between the hot gas and the cold molecular clouds. Zhu, Seaquist, & Kuno (2003) derived from CO measurements a pressure of 4.2×10^{-11} for the northern nucleus (NGC 4038) and of 3.1×10^{-11} dyne cm^{-2} for the southern nucleus (NGC 4039). Our observations suggest that the hot-gas pressure is a few times higher than the CO estimate for the northern nucleus and almost an order of magnitude higher in the southern nucleus. Such a large pressure difference would imply that shock waves are being driven into the CO clouds. The hot ISM may therefore in part be responsible for compressing and fragmenting the CO clouds, triggering star formation. However, we must bear in mind the large uncertainties in the estimated pressures, due to the assumptions we had to make on the emitting volume and the small-scale properties of the clouds.

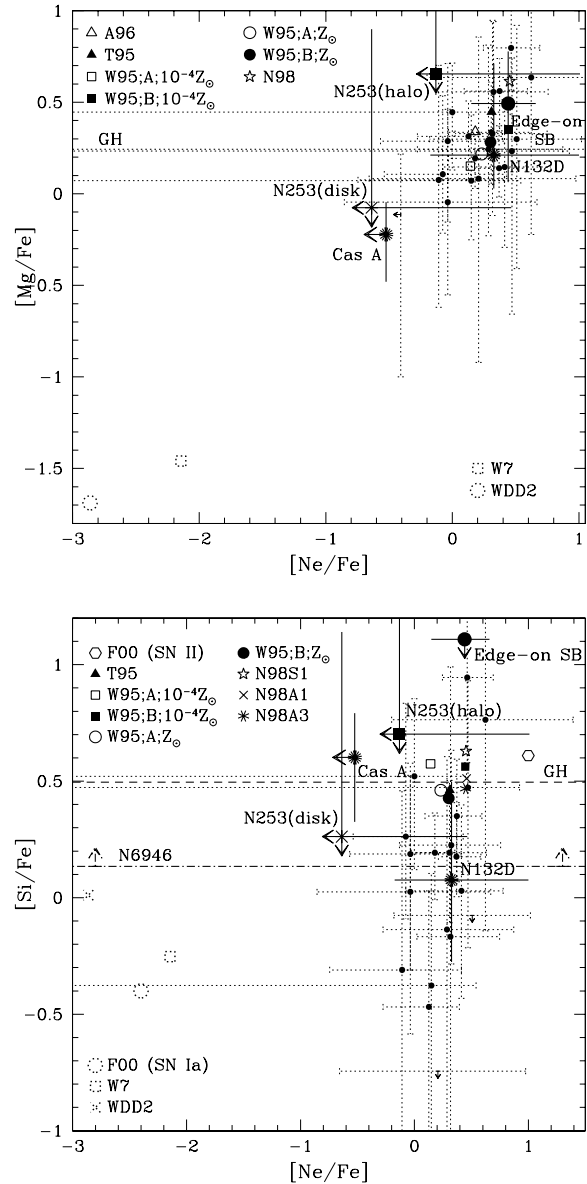


Figure 2. Abundance-ratio diagrams for regions of the Antennae hot ISM: $[\text{Ne}/\text{Fe}]$ vs. $[\text{Mg}/\text{Fe}]$ (left); $[\text{Ne}/\text{Fe}]$ vs. $[\text{Si}/\text{Fe}]$ (right). Abundance units refer to meteoritic abundances of Anders & Grevesse (1989). Each region is plotted with a small black dot (upper limits with black arrows). Dotted line symbols correspond to ratios expected in SNe Ia yields, while solid line symbols refer to the average stellar yield of SNe II. ‘‘F00’’ indicates values adopted in Finoguenov et al. (2000), while the other labels refer to the theoretical works listed in Nagataki & Sato (1998). Cas A and N132D SN ratios derived from the metallicities observed by BeppoSAX (Favata et al. 1997a, 1997b) are plotted too. Other symbols and lines refer to determinations of abundance ratios in other galaxies: the warm Galactic halo, NGC 253, NGC 6946 and the Strickland et al. (2004) sample of edge-on starbursts (see text for details).

4. ABUNDANCES

The elemental abundances of Ne-IX, Mg-XI, Si-XIII, and Fe-L that we measure in the hot ISM of The Antennae are generally consistent with the stellar abundances measured from optical data (~ 0.5 solar; Fritze-v. Alvensleben 1998), except for a few regions (4b, 5, 7, 8a and 8b) where the measured abundances are clearly in excess of this value and, in the case of Region 5, even significantly super-solar. While all the other regions have metallicities consistent with solar (within the errors), Region 5 is showing particularly enhanced abundances for three out of the four elements we measured ($Z_{Ne} > 3.9$, $Z_{Mg} > 3.8$, $Z_{Fe} > 1.3$, at 90% confidence level). Such high X-ray derived metallicities of Fe and especially of the α elements are quite rare and have been rarely found in previous observations of other galaxies (e.g. Soria & Wu 2002; Schlegel et al. 2003). This could be due both to the peculiarity of Region 5 and to the fact that constraining abundances through X-ray fitting of low resolution spectra is always a challenging task.

The ratios between elemental abundances in each region can be related to the type of supernovae generating the metals. If the elemental enrichment results from Type II supernovae, one would expect [Ne/Fe] and [Mg/Fe] values approaching 0.3, and [Si/Fe] values approaching 0.5 on average; the corresponding values expected in Type Ia supernova enrichment are dramatically lower (Nagataki & Sato 1998). We used our results to explore the origin of the metals in The Antennae. The [Ne/Fe], [Mg/Fe], and [Si/Fe] ratios of each spectral region are plotted in diagrams displaying the [Ne/Fe] ratio vs. [Mg/Fe] ratio and [Ne/Fe] vs. [Si/Fe] (Figure 2). In these diagrams, we also show the theoretical stellar yields expected from SNe Ia and SNe II, taken from the compilations by Finoguenov et al. (2000) and Nagataki & Sato (1998). We also indicate the regions occupied by the type-II supernova remnants (SNR) Cas A and N132D, using the abundances measured by Favata et al. (1997a,b) from BeppoSAX data. To relate our results to other measurements of these ratios in the literature we plot also the values relative to the warm Galactic halo (Savage & Sembach 1996), to the emission both from the disk and from the northern halo of NGC 253 (Strickland et al. 2002), to the X-ray diffuse emission observed in NGC 6946 (Schlegel et al. 2003), and to the averaged value in the hot halo of a sample of ten nearby edge-on starbursts (Strickland et al. 2004).

Although the uncertainties are often large, almost all regions observed in The Antennae show [Ne/Fe] and [Mg/Fe] ratios fully consistent with a SN II-dominated enrichment scenario. However, the [Si/Fe] ratio is clearly lower than expected in a SN II enrichment scenario, and in some cases it could be consistent with SN Ia enrichment, although the uncertainties are quite large also for this ratio. The only two exceptions to these trends are regions 5 and 7, both located in the upper right corners of the diagrams. These two regions have a [Si/Fe] ratio fully consistent with an enrichment stemming entirely from type-II supernovae.

Although our measurements are affected by large uncertainties they represent clearly an improvement over the

previous efforts aimed at measuring the α to Fe ratio in starburst galaxies. The only exception comes from the Strickland et al. (2004) sample of edge-on starburst galaxies. This data point, which has smaller error bars than our typical error bars, is consistent with the ratios observed in almost all the regions of The Antennae. However, note that their smaller error bars derive from the fact that they come from the observed hot halo emission in all ten galaxies of the sample. Moreover, in this sample they cannot put a stringent upper limit on the [Si/Fe] ratio, a thing that we were able to do in at least some of our regions.

4.1. X-ray abundances vs. Optical/Radio SF indicators

To further explore our results, we searched for correlations with age and star formation indicators for the different regions of The Antennae. NGC 4038/39 was observed by *HST*/WFPC2 (F336W, F439W, F555W, and F814W filters) in 1996 January (Whitmore et al. 1999). There were also VLA observations (in configurations BnA, CnB, and B at 6 and 4 cm) performed in 1997 January and 1998 September (Neff & Ulvestad 2000).

From the published data and our visual estimates it was possible to derive—for each region—four quantities that might correlate with ISM metal abundances: a mean cluster age, the relative strength of star formation, the star formation per unit area, and the number of SNRs per unit area. Details on how these quantities were calculated can be found in Baldi et al. (2005b).

Figure 3 displays the relations between the SF per unit area, SNRs per unit area and the mean abundance of α -elements in each region. There are no strong correlations between the different star-formation indicators we calculated and the mean abundances in the same regions. The “star-formation per unit area” and the number of “SNRs per unit area” are supposed to be among the best indicators of star formation. Yet, these two quantities appear uncorrelated with the metal abundances.

The hot-gas masses derived from the measure of the abundances may yield some clues toward an interpretation of this lack of correlations. Assuming the average SN II stellar yields listed in Nagataki & Sato (1998), we estimated the number of type-II SNe necessary to produce the observed metal masses in the hot ISM, and the time required to produce that number of SNe. If the resulting time is significantly shorter than 100 Myr, then the lack of correlations may either be related to the speed at which mixing occurs in the hot ISM or indicate that the metals are somehow removed from the hot phase of the ISM. Conversely, if the SN production time is ≥ 100 Myr, then mean cluster ages may not be relevant because over periods of 100 Myr or longer major fractions of the decaying galaxy orbits are traversed and it is unclear whether any relation could be established between regional abundances and the past local star-formation history.

A calculation for a range of theoretical models (see e.g. Nagataki & Sato 1998) for SN II average yields has been

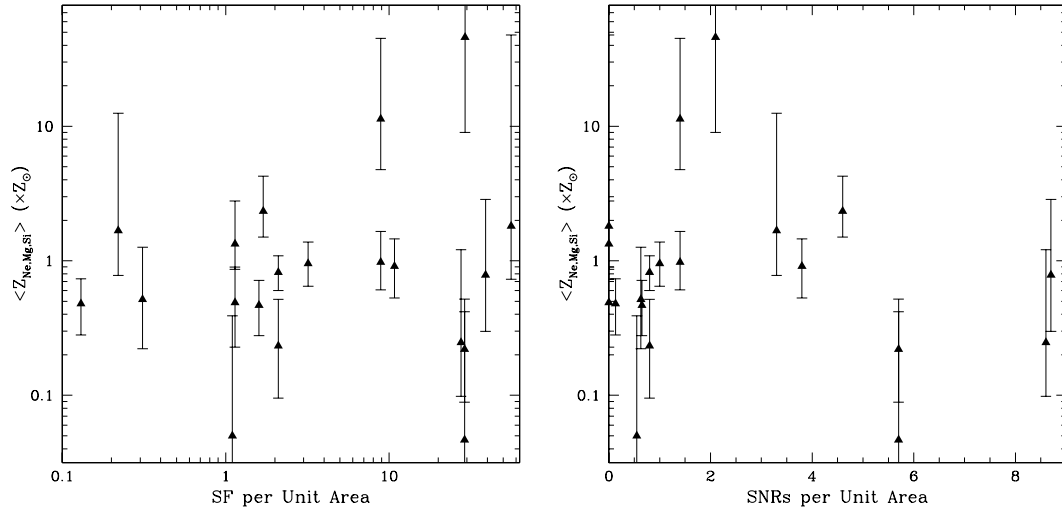


Figure 3. Diagrams of the mean abundances of α -elements in each spectral region of the Antennae hot ISM plotted versus star formation per unit area (left), and SNRs per unit area (right).

performed in Baldi et al. (2005b). In that paper, we estimated the time necessary to produce the required number of SNe II, assuming a constant SN rate throughout The Antennae. Neff & Ulvestad (2000) derived a SN rate directly associated with the compact radio sources detected in The Antennae of 0.03 yr^{-1} , assuming a typical SNR emits 6-cm radio emission for 30,000 yr and has the luminosity of Cas A. Applying instead the Condon & Yin (1990) method (based on the ratio of non-thermal radio luminosity to the radio-emitting SN rate in our Galaxy) to the total steep-spectrum radio emission of The Antennae, and not only to the detected compact sources, they predict a SN rate of 0.26 yr^{-1} . For both rate estimates the times required to produce the metals observed are quite short: in the $\sim 3.4\text{--}12 \text{ Myr}$ range for a SN rate of 0.03 yr^{-1} and in the $\sim 0.4\text{--}1.4 \text{ Myr}$ range for 0.26 yr^{-1} .

Indeed, 2 Myr is a relevant time threshold for mixing in a hot gas of the temperature we detect, corresponding to average velocities of $\sim 500 \text{ km s}^{-1}$. At 500 km s^{-1} , gas travels only $\sim 1 \text{ kpc}$ in 2 Myr. If the time required to produce the metals is actually of this order of $\leq 2 \text{ Myr}$, it may be unlikely that efficient mixing takes place on a scale larger than a few hundred pc, and it is probably insufficient to destroy the correlation. Other factors may have destroyed the correlation as well like, e.g., (i) the presence of a significant fraction of the SN ejecta in a cool phase or (ii) in dust grains, or (iii) the escape of the ejecta in a galactic wind. Another possibility could be that the other metals are invisible in soft X-rays. Indeed, in a Chevalier & Clegg (1985) wind model the metals would be expected to be in much hotter ($T \sim 10^{7.5} \text{ K}$) gas. Therefore the hot gas observed could be primarily ambient ISM heated, but not particularly enriched, by Type II SNe.

5. SUMMARY AND CONCLUSIONS

In this paper we described the main results of an extensive study of the X-ray properties of the diffuse emission of The Antennae (NGC 4038/39), analyzing the entire 411 ks exposure obtained with *Chandra* ACIS-S.

To summarize:

- 1) Fitting the Fe-L, Ne-IX, Mg-XI and Si-XIII emission for the hot ISM, we find significant metal enrichment. Metal abundances are generally consistent with solar, but reach extremes of ~ 20 solar in Region 5 and are significantly subsolar in a few regions.
- 2) We derived physical parameters of the hot gas, such as density, thermal energy, cooling times and pressure.
- 3) Comparison of elemental ratios with those expected from Type Ia and Type II SNe suggests that SNe II are mainly responsible for the metal enrichment of the hot ISM in The Antennae, although the measured [Si/Fe] ratios are mostly lower than those predicted for SN II yields. This may be due by poor data quality at the energy of the Si line ($E \sim 2 \text{ keV}$).
- 4) We report a remarkable lack of correlations between our abundance measurements and stellar age indicators, estimated from either the *Hubble* observations of stellar clusters (Whitmore & Schweizer 1995; Whitmore et al. 1999) or VLA SNR estimates (Neff & Ulvestad 2000). The time required to produce the observed quantities of metals through type-II SN explosions is probably $\leq 2 \text{ Myr}$, implying that efficient mixing is unlikely to be the main agent destroying the expected correlation between abundances and radio-optical star-formation indicators. This may point toward the presence of a significant fraction of SN II ejecta in a cool phase, in dust grains, or

escaping in a wind of hot gas, undetectable at soft X-rays wavelengths.

ACKNOWLEDGMENTS

We thank the *Chandra* X-ray Center DS and SDS teams for their efforts in reducing the data and for developing the software used in the data reduction (SDP) and analysis (CIAO). We thank D.-W. Kim for useful discussions. This work was supported in part by NASA contract NAS8-39073 and NASA grants GO1-2115X and GO2-3135X. F.S. acknowledges partial support from the NSF through grant AST 02-05994.

REFERENCES

- [1] Anders, E., & Grevesse, N. 1989, *Geochimica et Cosmochimica Acta*, 53, 197
- [2] Baldi, A., Raymond, J.C., Fabbiano, G., Zezas, A., Rots, A.H., Schweizer, F., King, A.R., Ponman, T.J. 2005a, *ApJS* in press (astro-ph/0410192)
- [3] Baldi, A., Raymond, J.C., Fabbiano, G., Zezas, A., Rots, A.H., Schweizer, F., King, A.R., Ponman, T.J. 2005b, *ApJ* in press (astro-ph/0509034)
- [4] Dahlem, M., Parmar, A., Oosterbroek, T., Orr, A., Weaver, K.A., Heckman, T.M. 2000, *ApJ*, 538, 555
- [5] de Avillez, M.A., & Breitschwerdt, D. 2004, *A&A*, 425, 899
- [6] Fabbiano, G., & Trinchieri, G. 1983, *ApJ*, 266, L5
- [7] Fabbiano, G., Schweizer, F., & Mackie, G. 1997, *ApJ*, 478, 542
- [8] Fabbiano, G., Zezas, A., Murray, S.S. 2001, *ApJ*, 554, 1035
- [9] Fabbiano, G., Krauss, M., Zezas, A., Rots, A., & Neff, S. 2003, *ApJ*, 598, 272
- [10] Fabbiano, G., Baldi, A., King, A.R., Ponman, T.J., Raymond, J., Read, A., Rots, A., Schweizer, F., & Zezas, A. 2004, *ApJ*, 605, L21
- [11] Favata, F., Vink, J., Parmar, A.N., Kaastra, J.S., & Mineo, T. 1997, *A&A*, 324, L45
- [12] Favata, F., Vink, J., dal Fiume, D., Parmar, A.N., Santangelo, A., Mineo, T., Preite-Martinez, A., Kaastra, J.S., & Bleeker, J.A.M. 1997, *A&A*, 324, L49
- [13] Finoguenov, A., David, L.P., & Ponman, T.J. 2000, *ApJ*, 544, 188
- [14] Fritze-v.Alvensleben, U. 1998, *A&A*, 336, 83
- [15] Gibson, B.K., Loewenstein, M., & Mushotzky, R.F. 1997, *MNRAS*, 290, 623
- [16] Heckman, T.M., 1999, *Ap&SS*, 266, 3
- [17] Hibbard, J.E., van der Hulst, J.M., Barnes, J.E., & Rich, R.M. 2001, *AJ*, 122, 2969
- [18] Martin, C.L., Kobulnicky, H.A., & Heckman, T.M. 2002, *ApJ*, 574, 663
- [19] McKee, C.F., & Ostriker, J.P. 1977, *ApJ*, 218, 148
- [20] Mirabel, I.F., Vigroux, L., Charmandaris, V., Sauvage, M., Gallais, P., Tran, D., Cesarsky, C., Maddus, S.C., & Duc, P.-A. 1998, *A&A*, 333, L1
- [21] Nagataki, S., & Sato, K. 1998, *ApJ*, 504, 629
- [22] Neff, S.G., & Ulvestad, J.S. 2000, *AJ*, 120, 670
- [23] Pudritz, R.E. & Fiege, J.D., 2000, in *ASP Conf. Series 168, New Perspectives on the Interstellar Medium*, A.R. Taylor, T.L. Landecker & G. Joncas, (San Francisco: ASP), 235
- [24] Read, A.M., Ponman, T.J., & Wolstencroft, R.D. 1995, *MNRAS*, 277, 397
- [25] Sansom, A.E., Dotani, T., Okada, K., Yamashita, A., & Fabbiano, G. 1996, *MNRAS*, 281, 48
- [26] Savage, B.D., & Sembach, K.R. 1996, *ARA&A*, 34, 279
- [27] Schlegel, E.M., Holt, S.S., & Petre, R. 2003, *ApJ*, 598, 982
- [28] Soria, R., & Wu, K. 2003, *A&A*, 410, 53
- [29] Strickland, D.K., Heckman, T.M., Weaver, K.A., Hoopes, C.G., & Dahlem, M. 2002, *ApJ*, 568, 689
- [30] Strickland, D.K., Heckman, T.M., Colbert, E.J.M., Hoopes, C.G., Weaver, K.A. 2004, *ApJS*, 151, 193
- [31] Weaver, K.A., Heckman, T.M., & Dahlem, M. 2000, *ApJ*, 534, 684
- [32] Weisskopf, M.C., O' Dell, S.L., & van Speybroeck, L.P. 1996, *SPIE*, 2805, 2
- [33] Whitmore, B.C., & Schweizer, F. 1995, *AJ*, 109, 960
- [34] Whitmore, B.C., Zhang, Q., Leitherer, C., Fall, S.M., Schweizer, F., & Miller, B.W. 1999, *AJ*, 118, 1551
- [35] Wilson, C.D., Scoville, N., Madden, S.C., & Charmandaris, V. 2000, *ApJ*, 542, 120
- [36] Zezas, A., Fabbiano, G., Rots, A.H., & Murray, S.S. 2002, *ApJS*, 142, 239
- [37] Zhang, Q., Fall, S.M., & Whitmore, B.C. 2001, *ApJ*, 561, 727
- [38] Zhu, M., Seaquist, E.R., & Kuno, N. 2003, *ApJ*, 588, 243